APPENDIX

Commercially available Head Impact Telemetry (HIT) System technology for American football (Sideline Response System, Riddell Inc., Chicago IL) acquires head acceleration data from six nonorthogonal, normally oriented, single-axis accelerometers fitted against a player's head. Traditionally, acceleration data acquired following head contact are post-processed with a simulated-annealing optimization algorithm that numerically iterates rigid-body dynamics equations to obtain peak linear acceleration magnitude at the head center of gravity.[3] Rotational acceleration is then calculated about two axes of rotation using the modeled equations of motion for force acting on the head, the anterior–posterior and medial–lateral components of the peak linear acceleration vector, and the directly measured relationship between linear and rotational acceleration for on-field head impacts.[13] As part of a multi-phase validation process, multiple laboratory assessments of the HIT System have been conducted to verify accuracy and precision of these processing and data reduction techniques.[2, 3, 6, 10]

As available, these data are insufficient input to finite element head models, which require independent temporal components of both linear and rotational acceleration about the head center of gravity to estimate brain tissue response following impact. To overcome this limitation, recorded acceleration data for each head impact in the accompanying study was post-processed using a custom, six degree of freedom expanded processing algorithm (6DOF-EPA). The development of 6DOF-EPA, which is based on a technique previously verified and implemented in research-only HIT System variants that utilized tangentially oriented accelerometers (i.e. boxing, soccer, ice hockey, and football), is described below.[1, 3, 7, 12] To verify accuracy of this approach, previously published HIT System experimental data obtained through laboratory testing was reprocessed and compared to acceleration data measured by a Hybrid III (HIII) anthropomorphic test device.[2]

Expanded Processing Algorithm

6DOF-EPA directly solves for linear and rotational head accelerations about the head center of gravity using data obtained from six accelerometers placed normal to the surface of the head. By assuming rigid body dynamics, the acceleration of any point (*i*) on the head ($\vec{a}_i$) undergoing linear and rotational acceleration is projected on the sensing axis of the accelerometer ($\vec{r}_{ai}$):

$$\|a_i\| = \vec{r}_{ai} \cdot \vec{H} + \vec{r}_{\dot{a}} \cdot (\vec{\alpha} \times \vec{r}_i) + \vec{r}_{\dot{a}} \cdot \left(\vec{\omega}_i \times (\vec{\omega}_i \times \vec{r}_i)\right) \quad (1)$$

where $\vec{H}$ is the linear acceleration vector at the head center of gravity (CG), $\vec{r}_i$ is the position vector of point *i* relative to head CG, $\vec{\alpha}$ is the rotational acceleration of the head, and $\vec{\omega}$ is the angular velocity of the head. Iterative optimization can then be used to solve for the linear acceleration ($\vec{H}$), rotational acceleration (α), and rotational velocity (ω) that minimizes the sum of square error between each accelerometer value and the expected acceleration:

$$\min \sum_{i=1}^{n} \left[\|a_i\| - \vec{r}_{ai} \cdot \vec{H}_E + \vec{r}_{\dot{a}} \cdot (\vec{\alpha}_E \times \vec{r}_i) + \vec{r}_{\dot{a}} \cdot \left(\vec{\omega}_E \times (\vec{\omega}_E \times \vec{r}_i)\right)\right]^2 \quad (2)$$

where *n* is the number of accelerometers, $\vec{H}_E$ is the estimated linear acceleration of the head CG, and $\vec{\alpha}_E$ and $\vec{\omega}_E$ are the estimated rotational acceleration and velocity vectors, respectively.

For the commercially available HIT System processing algorithm, rotational and centripetal acceleration is neglected based on an assumption that the accelerometer sensing axis is not radially oriented to the acceleration vector. Additionally, a single optimization is performed at the time of peak acceleration. Thus reducing Equation 2 to the following:

$$\min \sum_{i=1}^{n} \left[\|a_i\| - \vec{r}_{ai} \cdot \vec{H}_k \right]^2 \quad (3)$$

where k is a discrete point in time (e.g. time of peak acceleration). While not accounting for rotational components contributes to overall measurement error and reducing the number of optimizations limits temporal resolution, this assumption provides a robust optimization solution and an acceptable level of measurement accuracy and processing time for on-field use.[2]

For 6DOF-EPA, a piecewise processing procedure was adopted to maintain established accuracy and integrity of peak linear acceleration measurements, obtain X, Y, and Z linear acceleration time series, and directly solve for X, Y, and Z rotational acceleration. Three serial processing steps were created to obtain: *1) Peak Linear Head Acceleration* – Single iterative optimization of Equation 3 to solve for peak linear head acceleration and impact location, *2) Linear Acceleration Time Series* – Iterative optimizations of Equation 3 for discrete points in time. For the HIT System, which records 40 ms of data at 1000 Hz, this requires 40 optimizations for a single head impact. Peak linear acceleration obtained from Step 1 is included as a known optimization parameter, and *3) Rotational Acceleration Time Series* - Iterative optimizations of Equation 2 for each discrete point in time. Centripetal acceleration is considered negligible, and temporal components of linear acceleration obtained from Step 2 are included as known parameters. While computationally taxing (i.e. 81 optimizations for a single head impact), this approach best leverages available information obtained from the HIT System hardware to obtain the independent, temporal linear and rotational head acceleration data required for FEBM.

Experimental Data

Laboratory reconstructions were previously conducted to correlate head impact kinematics recorded by the commercially available HIT System and an instrumented Hybrid III headform under conditions that simulated impact velocities and locations associated with National Football League head impacts.[2] Four impact sites, designated as A, B, C, and D, were impacted with a pneumatic linear ram at four target speeds (4.4, 7.4, 9.3, and 11.2 m/s) to represent on-field impacts associated with and without concussion (Figure 1). Three to five trials were conducted at each site and speed, resulting in 54 impacts available for review.

Acceleration data obtained from the HIT System for each impact was post-processed with 6DOF-EPA, providing X, Y, and Z components of both linear and rotational acceleration.

Resultant time series were calculated from component data, and peak measures were defined by the maximum time series acceleration. Corresponding HIII acceleration data, which was obtained from 9 accelerometers positioned in a 3-2-2-2 configuration was unchanged from previous published reports.[2, 11] Direction was defined for both measurement devices following right-hand rule in a fixed Cartesian coordinate system at the head center of gravity (i.e. positive X direction towards the front of the head, positive Y towards the left ear, and positive Z towards the top of the head).

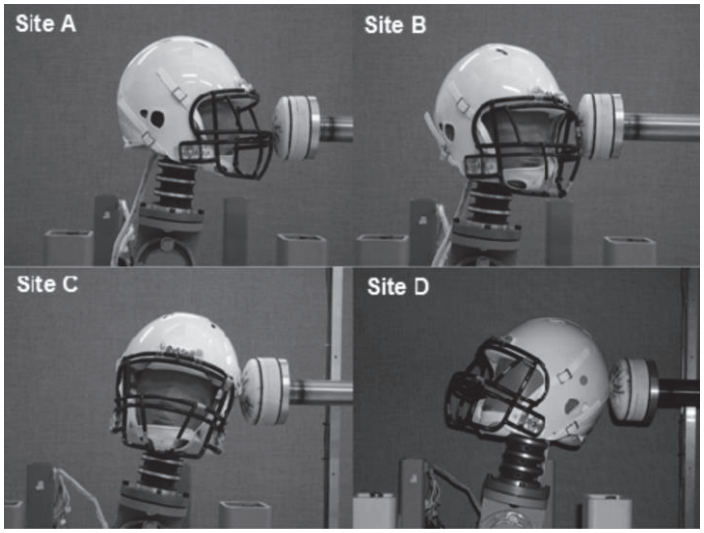

Figure 1 Four primary impact sites were (A, B, C, and D) were identified as points of contact that most frequently result in mTBI for NFL athletes. Each site was impacted at four target speeds: 4.4, 7.4, 9.3, and 11.2 m/s.

Verifying Accuracy of 6DOF-EPA Peak Output

Following methods described in the previous evaluation, linear regression analysis was performed to assess correlation between peak linear and angular acceleration measures from the 6DOF-EPA and HIII. As described in the previous evaluation, all regressions were performed both on the entire data set and by impact site using equation 4:

$$y = mx + y_0 \quad (4)$$

where x is the HIII measure, y is the HIT System measure, and the linear slope, m, is the

Table 1 Results from linear regression analysis between HIT System and HIII impact measures. The relationship between measures (m) and coefficient of determination (r^2) are shown for peak accelerations obtained at all impact sites. Previously published results when using commercially available HIT System processing are included for reference.[2]

	A		B		C		D		Overall A-B-C-D	
	m	r^2	*m*	r^2	*m*	r^2	*m*	r^2	*m*	r^2
Linear Acc. (historical)	1.055	0.930	0.995	0.822	1.084	0.987	0.969	0.875	**1.009**	**0.903**
Linear Acc. (6DOF – EPA)	1.055	0.930	0.995	0.822	1.084	0.987	0.969	0.875	**1.009**	**0.903**
Rotational Acc. (historical)	0.549	0.415	0.917	0.961	1.170	0.981	1.125	0.710	**0.939**	**0.528**
Rotational Acc. (6DOF-EPA)	0.770	0.726	0.895	0.930	1.047	0.974	1.050	0.608	**0.942**	**0.718**

relationship between the measurements. For all conditions, y_0 was constrained to be zero since both systems have a baseline output of zero when not impacted. The coefficient of determination (r^2) was also calculated for each regression as a measure of goodness of fit. Slopes of the fit trendlines and coefficients of determination are summarized in Table 1. For reference, previously published results obtained with the commercially available HIT System processing algorithm are included. As defined, there was no change in peak linear acceleration. Modestly higher correlations were obtained for peak rotational acceleration, with the largest improvement occurring at the A impact site.

Verifying Biofidelity of 6DOF-EPA Temporal Output

The Normalized Integral Square Error (NISE) was developed to quantitatively measure the similarity of time history response produced by two anthropomorphic test devices.[5] It has since been employed by FE model developers to assess biofidelity of model estimated tissue response with direct measurements obtained through experimental methods.[4, 8, 9] A detailed account of these calculations and their derivation has been previously described.[4, 5, 9]

Briefly, the NISE method is used to evaluate three aspects of time history curves - amplitude difference (N-amp), shape difference (N-shape), and phase shift (N-phase). Because the NISE method produces Error Measures (EM) that are equal to zero when strong correlation exits, it has become common practice to calculate a Correlation Score (equation 5) that range from 0 to 100, with higher scores equating to higher correlation.

$$CS_{N-amp} = 100 \times \left(1 - \left|EM_{N-amp}\right|\right) \quad (5)$$

Correlation scores can then be used to classify performance according to the following biofidelity rating:[4, 9]

Excellent:	86 ≤ CS < 100
Good:	65 ≤ CS < 86
Fair:	44 ≤ CS < 65
Marginal:	26 ≤ CS < 44
Unacceptable:	0 ≤ CS < 26

For this analysis, CS were calculated for all component and resultant accelerations and grouped by impact site. Only $CS_{N\text{-}amp}$ and $CS_{N\text{-}shape}$ were considered, as simultaneous triggering of the two measurement systems was not feasible in the experimental design.

Overall, average CS values indicated excellent correlation for all component and resultant acceleration time series except for the shape of rotational acceleration in the Z direction which was in the marginal biofidelity range (Table 2). Marginal correlation for Z rotation shape was due primarily to relatively small Z acceleration contributions at A, B, and C sites where rotation occurred primarily about the X and Y axes. This was especially the case for low velocity impacts, as indicated by the high within-site standard deviations observed. For all other impact sites,

component and resultant CS had excellent to good biofidelity except for $CS_{N\text{-}amp}$ linear acceleration in the C direction which had fair correlation. Again, reduced correlation was due primarily to minimal linear acceleration contribution in the X direction for side of the head impacts.

Table 2 Mean and standard deviation of CS values for linear and rotational acceleration at the head center of gravity.

	A		**B**		**C**		**D**		**Overall A-B-C-D**	
	$CS_{N\text{-}amp}$	$CS_{N\text{-}shape}$	$CS_{N\text{-}amp}$	$CS_{N\text{-}shape}$	$CS_{N\text{-}amp}$	$CS_{N\text{-}shape}$	$CS_{N\text{-}amp}$	$CS_{N\text{-}shape}$	$CS_{N\text{-}amp}$	$CS_{N\text{-}shape}$
Linear Acc.										
X dir.	98.82 (1.80)	99.46 (1.88)	92.58 (3.90)	80.84 (17.62)	61.43 (6.83)	100.00 (0.01)	92.72 (3.86)	99.56 (0.47)	**87.09 (14.70)**	**95.47 (11.30)**
Y dir.	82.54 (22.38)	98.12 (3.68)	99.30 (0.91)	99.82 (0.44)	99.63 (0.48)	99.60 (0.58)	91.86 (7.89)	99.97 (0.09)	**93.17 (12.97)**	**99.44 (1.86)**
Z dir.	91.24 (5.53)	96.28 (7.38)	88.55 (7.81)	100.00 (0.00)	93.21 (8.82)	97.70 (4.48)	91.41 (10.84)	75.54 (10.98)	**91.14 (8.68)**	**90.51 (13.03)**
Resultant	95.63 (3.59)	98.92 (2.20)	97.52 (2.13)	99.60 (0.80)	97.47 (3.17)	99.93 (0.16)	96.15 (2.24)	99.93 (0.13)	**96.63 (2.82)**	**99.64 (1.15)**
Rotational Acc.										
X dir.	80.10 (18.88)	99.71 (0.69)	95.71 (4.56)	100.00 (0.00)	99.17 (0.80)	99.93 (0.14)	96.43 (4.02)	100.00 (0.00)	**93.25 (11.64)**	**99.92 (0.34)**
Y dir.	98.48 (2.11)	61.96 (21.15)	91.37 (16.06)	97.02 (4.62)	86.56 (9.85)	91.62 (11.31)	88.23 (8.87)	99.90 (0.19)	**90.84 (10.93)**	**88.99 (18.60)**
Z dir.	85.33 (15.01)	18.04 (43.28)	97.88 (2.65)	53.57 (24.44)	79.51 (10.22)	49.82 (19.13)	94.29 (3.76)	93.46 (5.89)	**89.81 (11.16)**	**34.33 (60.42)**
Resultant	91.58 (9.31)	97.97 (4.68)	99.55 (0.59)	86.81 (9.45)	95.05 (3.63)	99.67 (0.73)	95.83 (2.51)	99.99 (0.02)	**95.54 (5.49)**	**96.54 (7.17)**

1. Beckwith, J. G., J. J. Chu, and R. M. Greenwald. Validation of a noninvasive system for measuring head acceleration for use during boxing competition. J Appl Biomech. 23(3):238-244, 2007.
2. Beckwith, J. G., R. M. Greenwald, and J. J. Chu. Measuring head kinematics in football: Correlation between the Head Impact Telemetry System and Hybrid III headform. Ann Biomed Eng. 40(1):237-248, 2012.
3. Crisco, J. J., J. J. Chu, and R. M. Greenwald. An algorithm for estimating acceleration magnitude and impact location using multiple nonorthogonal single-axis accelerometers. J Biomech Eng. 126(6):849-854, 2004.
4. de Lange, R., L. van Rooij, H. Mooi, and J. Wismans. Objective biofidelity rating of a numerical human occupant model in frontal to lateral impact. Stapp Car Crash J. 49(November):457-479, 2005.
5. Donnelly, B. R., R. M. Morgan, and R. H. Eppinger. Durability, repeatability and reproducibility of the nhtsa side impact dummy. Tweny-seventh Stapp Car Crash Conference Proceedings. San Diego, California. 299-310, 1983.
6. Duma, S. M., S. J. Manoogian, W. R. Bussone, P. G. Brolinson, M. W. Goforth, J. J. Donnenwerth, R. M. Greenwald, J. J. Chu, and J. J. Crisco. Analysis of real-time head accelerations in collegiate football players. Clin J Sport Med. 15(1):3-8, 2005.
7. Hanlon, E., and C. Bir. Validation of a wireless head acceleration measurement system for use in soccer play. J Appl Biomech. 26(4):424-431, 2010.
8. Ji, S., W. Zhao, J. C. Ford, J. G. Beckwith, R. P. Bolander, R. M. Greenwald, L. A. Flashman, K. D. Paulsen, and T. McAllister. Group-wise evaluation and comparison of white matter fiber strain and maximum principal strain in sports-related concussion. J Neurotrauma. 32(7):441-454, 2015.
9. Kimpara, H., Y. Nakahira, M. Iwamoto, and K. Miki. Investigation of anteroposterior head-neck responses during severe frontal impacts using a brain-spinal cord complex fe model. Stapp Car Crash J. 50(November):509-544, 2006.
10. Manoogian, S., D. McNeely, S. Duma, G. Brolinson, and R. Greenwald. Head acceleration is less than 10 percent of helmet acceleration in football impacts. Biomed Sci Instrum. 42:383-388, 2006.
11. Padgaonkar, A. J., K. W. Krieger, and A. I. King. Measurement of angular accelerations of a rigid body using linear accelerometers. Journal of Applied Mechanics. 42(3):552-556, 1975.
12. Rowson, S., J. G. Beckwith, J. J. Chu, D. S. Leonard, R. M. Greenwald, and S. M. Duma. A six degree of freedom head acceleration measurement device for use in football. J Appl Biomech. 27(1):8-14, 2011.
13. Rowson, S., S. M. Duma, J. G. Beckwith, J. J. Chu, R. M. Greenwald, J. J. Crisco, P. G. Brolinson, A. C. Duhaime, T. W. McAllister, and A. C. Maerlender. Rotational head kinematics in football impacts: An injury risk function for concussion. Ann Biomed Eng. 40(1):1-13, 2012.